# Third-order nonlinear optical properties of Ge-As-Te chalcogenide glasses in mid-infrared

Li, Qiuli; Wang, Rongping; Xu, Fu; Wang, Xunsi; Yang, Zhiyong; Gai, Xin

**Published in:**
Optical Materials Express

**Published: 01/06/2020**

**Document Version:**
Final Published version, also known as Publisher's PDF, Publisher's Final version or Version of Record



**Published version (DOI):**
10.1364/OME.392655

**Publication details:**
Li, Q., Wang, R., Xu, F., Wang, X., Yang, Z., & Gai, X. (2020). Third-order nonlinear optical properties of Ge-As-Te chalcogenide glasses in mid-infrared. *Optical Materials Express*, *10*(6), 1413-1420. https://doi.org/10.1364/OME.392655

Research Article | Vol. 10, No. 6 / 1 June 2020 / Optical Materials Express 1413
Optical Materials EXPRESS

# Third-order nonlinear optical properties of Ge-As-Te chalcogenide glasses in mid-infrared

Qiuli Li,[1,2] Rongping Wang,[1,5] Fu Xu,[3] Xunsi Wang,[1] Zhiyong Yang,[3] and Xin Gai[2,4,6]

[1]Laboratory of Infrared Materials and Devices, Research Institute of Advanced Technologies, Ningbo University, Ningbo 315211, China
[2]Department of Electrical Engineering, City University of Hong Kong, 83 Tat Chee Avenue, Kowloon, Hong Kong SAR, China
[3]Jiangsu Key Laboratory of Advanced Laser Materials and Devices, School of Physics and Electronic Engineering, Jiangsu Normal University, Xuzhou, Jiangsu 221116, China
[4]State Key Lab of Terahertz and Millimeter Waves, City University of Hong Kong, 83 Tat Chee Avenue, Kowloon, Hong Kong SAR, China
[5]wangrongping@nbu.edu.cn
[6]xingai@cityu.edu.hk

**Abstract:** Third-order nonlinear optical properties of $Ge_{10}As_xTe_{90-x}$ chalcogenide glasses were investigated utilizing the Z-scan method at the mid-infrared wavelengths of 2.5 and 3.0 μm. The compositional dependence of the third-order nonlinearity was analyzed, and their correlation with the refractive index and the optical bandgap was discussed. The results show that nonlinear refractive index $n_2$ can be significantly enhanced by the addition of tellurium, and larger $n_2$ values are observed at 3.0 μm rather than 2.5 μm due to the two-photon resonance effect, and the maximum of $n_2$ is $4.96 \times 10^{-13}$ $cm^2/W$ at the composition of $Ge_{10}As_{20}Te_{70}$. In addition, the experimental results are in good agreement with the semi-empirical Miller's rule whilst the variation of dispersive $n_2$ values are in relatively good coincidence with the theoretical model by Sheik-Bahae et.al. for direct bandgap semiconductors.



## 1. Introduction

Chalcogenide glasses, consisting of one or more chalcogen elements including S, Se, and Te that are covalently bonded with the other glass-forming elements like Ge, As, Sb etc., possess ultrahigh third-order optical nonlinearity $\chi^{(3)}$ and broadband optical transmittance [1,2], thus are promising for various mid- & far-infrared photonic applications, such as environmental monitoring, biomedical sensing, energy research and supercontinuum generation [3–8]. For these applications, it is essential to investigate nonlinear optical properties of chalcogenide glasses for optimized compositions in the mid-infrared. This has been intensively performed in As-S-Se, Ag-As-Se, Ge-As-S(Se) and Ge-Sb-S(Se) [9–15], and several semi-empirical semiconductor models have been developed to predict the correlations of the optical nonlinearities with the other material properties such as optical bandgap energy $E_g$ and linear refractive index $n_0$. However, the transmission spectrum of S- and Se-based chalcogenide glasses is barriered at 12 μm and 15 μm, respectively [16,17], whilst extended long-wave transmission towards the far-infrared is sought by the emerging applications in environmental, biomedical, energy and astronomical sectors. By contrast, Te-based chalcogenide glasses are capable of exceptional long-wave transmission beyond 20 μm since Te is heavier element in contrast to S and Se, leading to lower lattice vibrational phonon energies [16,17]. Besides the outstanding long-wave transmission property, the advantages of Te-based chalcogenide glasses also include the highly linear refractive index for strong light confinement of photonic circuits, the significant nonlinear refractive index for all-optical signal processing [1,18] rapid reversible transition between crystalline and amorphous

#392655 https://doi.org/10.1364/OME.392655
Journal © 2020 Received 13 Mar 2020; revised 3 May 2020; accepted 12 May 2020; published 19 May 2020

Optical Materials EXPRESS

status for optical data storage [19] and so on. However, Te-based chalcogenide glasses have narrow glass-forming region, for example, $Ge_xTe_{1-x}$ chalcogenide can only form bulk glasses in a range of $15 < x < 20$ [20,21], thus the compositional tuneability for improved optical properties is restrained.

By adopting As into Ge-Te chalcogenide system, the glass-forming region of the ternary $Ge_xAs_yTe_{1-x-y}$ glass system is then extended so that the content of Ge can change from 0 to 15% and that of As is variable between 10% and 50%, so that screening the glass compositions for optimized nonlinear optical properties becomes possible in the ternary glass system. In this work, we set the Ge content as a constant value of 10 mol% and thus $Ge_{10}As_xTe_{90-x}$ glasses with a varied As content from 15% to 55% were investigated for the correlations of As contents with the linear and nonlinear optical properties. The optical properties of the $Ge_{10}As_xTe_{90-x}$ glasses like optical bandgap energy, refractive index and transmission spectra were investigated by using infrared spectroscopy and ellipsometer whilst the nonlinearities were characterized by using mid-infrared Z-scan method at the wavelengths of 2.5 μm and 3.0 μm. The dependence of nonlinear index on linear refractive index and the correlation of the dispersive nonlinearities with the optical bandgap energies were systemically analyzed following by the theorical predictions from the semi-empirical models.

## 2. Experiment

The bulk glasses were synthesized via the melt-quenching method from elemental Ge, As, and Te with 5N purity. The starting materials were weighted and then introduced into fused silica ampoules with an internal diameter of 10 mm. The ampoules were sealed under vacuum of $10^{-3}$ Pa, then placed into a rocking furnace homogenizing for no less than 12 h at 900 °C, and eventually quenched by cold water. In order to release the inner stress, the glass boules were subsequently annealed at 15°C below the glass transition temperature $T_g$ for 5 h and then slowly cooled at a rate of 10°C/h to room temperature.

The transmission spectra of the glasses were characterized by utilizing a spectrometer (Lambda 950, PerkinElmer) in visible and near infrared region and a Fourier transform infrared spectrometer (Nicolet 380, Thermo Scientific) in a spectral range between 2.5 and 25 μm. The refractive index was measured by using an infrared variable angle spectroscopic ellipsometer (IR-VASE, J. A. Woollam, Lincoln, NE) ellipsometry in the range between 1.7-20 μm and was processed by using Cauchy model that had widely used for chalcogenide glasses.

For preparing the Z-scan samples, the glass boules were sectioned to flat disks of 1.0 mm thickness and then polished to optical quality. The Z-scan pump light was ~170 fs pulses generated from an optical parametric amplifier (Orpheus-HP, Light Conversion, Lithuania) pumped by an Yb: KGW laser at a repetition rate of 100 kHz. To inhibit the scattering noise due to the laser instability, the pump light was split into two beams, so as one of the beams was monitored by a HgCdTe detector (S180C, Thorlabs, USA) as the reference light, and the other one was focused into gaussian beam by a 30 cm focal length optical lens as the pump light that was detected by another HgCdTe detector.

Z-scan technique was implemented to characterize both the nonlinear index and two-photon absorption of the Te-based chalcogenide glasses. The close aperture measurement acquires the nonlinear phase change information whilst the open aperture experiment is in regard to the two-photon nonlinear absorption. Because the two-photon absorptions of $Ge_xAs_yTe_{1-x-y}$ glasses were not negligible, we had to adopt the Z-scan fitting equations so that the influence of two-photon absorption was contemplated for the close aperture experimental results [22,23],

$$T_{CA} = 1 + \frac{4x}{(x^2+9)(x^2+1)}\Delta\Phi_0 - \frac{1}{\sqrt{2}(x^2+1)}\Delta\Psi_0 \tag{1}$$

Optical Materials EXPRESS

$$T_{OA} = 1 - \frac{1}{\sqrt{2}(x^2+1)}\Delta\Psi_0 \tag{2}$$

where $\Delta\Phi_0$ is the nonlinear phase shift and $\Delta\Psi_0$ is the two-photon induced absorption. The $x = z_0 = 2z/k{\omega_0}^2$ is the sample displacement from the focusing plane position, $z$ is the real time sample position and $k$ is the wave vector of the light. The beam waist $\omega_0$ was 26 μm at 2.5 μm wavelength and 32 μm at 3.0 μm. Notably, the error bar of beam waist measurement was estimated to be 15%. Subsequently, the nonlinear refractive index $n_2$ and two photon absorption $\beta$ can be derived from,

$$\Delta\Phi_0 = Kn_2I_0L_{eff} \tag{3}$$

$$\Delta\Psi_0 = \beta I_0 L_{\text{eff}}/2 \tag{4}$$

where $I_0$ is the laser intensity in the focus, $L_{eff}$ is the effective thickness of the glasses that is determined by $L_{eff}$ =[1-exp(−α$L$)]/$\alpha$, in which $L$ is the thickness of the glasses and $\alpha$ is the linear absorption coefficient.

Figures 1(a)-(b) show the close aperture measurement on composition of $Ge_{10}As_{20}Te_{70}$ glass at 2.5 and 3.0 μm respectively. These signals of all $Ge_{10}As_xTe_{90-x}$ glass samples show similarities to each other: the pre-focal valley followed by a post-focal peak indicates a positive $n_2$ due to self-focusing effect, whilst the gaps between valley and peak represent the value of the nonlinear phase change induced by the pulsed laser in the samples that is used to determine the nonlinear refractive index of the materials. Figure 1(c) is the open aperture measurement for varied As content compositions at 3.0 μm. The relation of the nonlinear absorption $Ln(1\text{-}T_{OA})$ versus peak irradiance $Ln(I_0)$ is demonstrated in Fig. 1(d) in which a linear fitting with slope of 1.07 indicates that the dominant nonlinear absorption at the investigated wavelength is two-photon absorption [24].

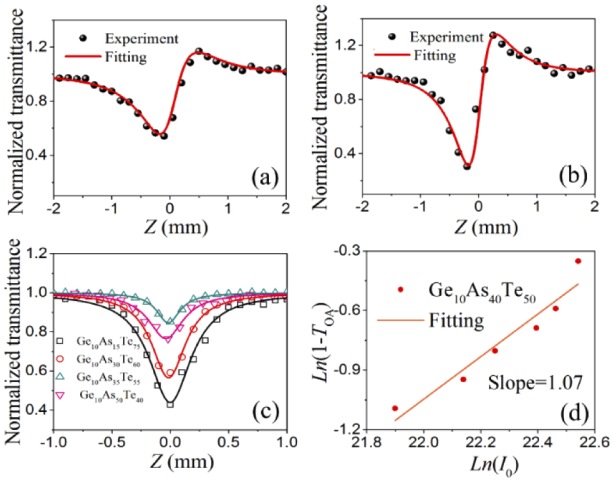


**Fig. 1.** Closed-aperture Z-scans measurement and fittings for $Ge_{10}As_{20}Te_{70}$ at 2.5 μm (a) and at 3.0 μm (b). (c) The open aperture measurement and the fitting for four compositions. (d) The linear fitting of $Ln(1\text{-}T_{OA})$ vs peak irradiance $Ln(I_0)$. The slope of the fitting line determines the two-photon absorption.

## 3. Results and discussion

Figure 2 shows the transmission spectrum and linear refractive index for a Te-based chalcogenide glass with composition of $Ge_{10}As_{20}Te_{70}$. The other compositions of this series of glasses show

Optical Materials EXPRESS

similar transmittances except the shifts on the short transmission edges due to the variation of optical bandgap energies. The values of linear index of Te-based chalcogenide are as high as >3.6 in mid-infrared leading to significant light confinement and manipulation capabilities. Such values are also in agreement with the reported values in Ref. [25].

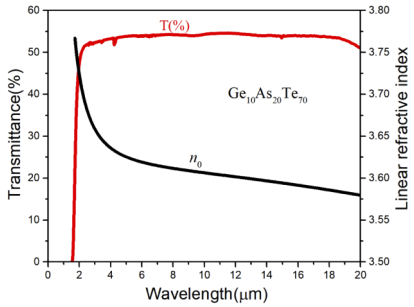


**Fig. 2.** Optical transmittance spectrum and linear of refractive index dispersion for $Ge_{10}As_{20}Te_{70}$ glass.

The optical band gap ($E_g$) was derived from the Tauc plots [26] using ultrathin glass samples with a thickness of 10-50 μm prepared by the hot-pressing method [27]. All the results were summarized in Table 1. The increase of Te content coincides with the decrease in $E_g$ that is consistent with previous reports in Ge-Se-Te [18] and Ge-Se-Sb-Te [28] glasses. In chalcogenide glasses, usually the valence bands are dominated by the lone-pair electrons whilst the conduction bands are related to the antibonding orbitals [29]. Consequently, $E_g$ decreases with the Te content because of the increase of Te-induced lone-pair electrons in the valence band so as rising of the highest occupied molecular orbital states [30].

**Table 1. Bandgap energy ($E_g$), refractive index ($n_0$), nonlinear refractive index ($n_2$), two-photon absorption coefficient (β) and *FOM* = $n_2/\beta\lambda$ at 2.5 and 3.0 μm, respectively, for $Ge_{10}As_xTe_{90-x}$ glasses.**

| Composition (in mol.%) | $E_g$ (±0.01eV) | $n_0$ (±0.01) | $n_2(10^{-13}$ cm$^2$/W) ±15% | $\beta$(cm/GW) ±15% | *FOM* ($n_2/\beta\lambda$) | $n_0$ (±0.01) | $n_2(10^{-13}$ cm$^2$/W) ±15% | $\beta$(cm/GW) ±15% | *FOM* ($n_2/\beta\lambda$) |
|---|---|---|---|---|---|---|---|---|---|
| | | | 2.5 μm | | | | 3.0 μm | | |
| $Ge_{10}As_{55}Te_{35}$ | 0.84 | 3.63 | 1.20 | 2.44 | 0.20 | 3.57 | 1.90 | 2.00 | 0.32 |
| $Ge_{10}As_{50}Te_{40}$ | 0.82 | 3.60 | 1.34 | 2.44 | 0.22 | 3.55 | 1.97 | 2.06 | 0.32 |
| $Ge_{10}As_{40}Te_{50}$ | 0.80 | 3.63 | 1.34 | 2.59 | 0.21 | 3.59 | 3.02 | 2.68 | 0.38 |
| $Ge_{10}As_{35}Te_{55}$ | 0.81 | 3.66 | 1.39 | 2.50 | 0.22 | 3.61 | 3.16 | 1.70 | 0.62 |
| $Ge_{10}As_{30}Te_{60}$ | 0.77 | 3.72 | 1.79 | 3.18 | 0.23 | 3.67 | 4.67 | 3.55 | 0.44 |
| $Ge_{10}As_{25}Te_{65}$ | 0.75 | 3.68 | 1.76 | 2.97 | 0.24 | 3.63 | 4.61 | 3.00 | 0.51 |
| $Ge_{10}As_{20}Te_{70}$ | 0.74 | 3.67 | 2.49 | 5.41 | 0.18 | 3.66 | 4.96 | 3.34 | 0.50 |
| $Ge_{10}As_{15}Te_{75}$ | 0.72 | 3.66 | 2.04 | 5.64 | 0.14 | 3.64 | 4.62 | 4.42 | 0.35 |

In Table 1, the overall $n_2$ values are above $10^{-13}$ cm$^2$/W with a maximum value of 4.96 $\times 10^{-13}$ cm$^2$/W at 3.0 μm. In comparison, $As_2S_3$, $Ge_{11.5}As_{24}Se_{65.5}$ and AMTIR-1 chalcogenide glasses are reported of $n_2$ values between $3.02\times10^{-14}$ cm$^2$/W and $8.31\times10^{-14}$ cm$^2$/W at 1.55 μm whilst their $n_2$ values further decrease with increasing wavelengths [10–12,27,31]. So the maximum of $n_2$ value for $Ge_{10}As_xTe_{90-x}$ glasses at 3.0 μm is 5 to 15 times higher than those in the other chalcogenide glasses such as $As_2S_3$, $Ge_{11.5}As_{24}Se_{65.5}$ and AMTIR-1, even taking their $n_2$ value at 1.55 μm Meanwhile, significant enhancement of $n_2$ is observed when the pump wavelength

Optical Materials EXPRESS

varies from 2.5 μm to 3.0 μm that is the evidence of two-photon resonance effect at the photon energies approaching the half of the bandgap energies.

Figures 3(a)-(c) show linear refractive index $n_0$, nonlinear refractive index $n_2$ and two-photon absorption coefficient $\beta$ of $Ge_{10}As_xTe_{90-x}$ glasses as functions of As content, respectively. According to Raman scattering [32,33] and x-ray photoelectron spectroscopy analysis [34], with increasing As content x in $Ge_{10}As_xTe_{90-x}$ glasses, the numbers of Te-Te-Te trimmers and Te-Te-As(Ge) structural units decrease and finally disappear, while the perfect $AsTe_{3/2}$ pyramidal and $GeTe_{4/2}$ tetrahedral structure in Te-rich samples gradually transferred to defect structures including As-As and Ge-Ge homopolar bonds at x = 50. Therefore, the maximum and minimum values of $n_0$ at x = 30 and 50 as shown in Fig. 3(a), appear to correspond to the chemical stoichiometric structure of $Ge_{10}As_{28}Se_{62}$ ($\{GeTe_2\}_{0.1}$-$\{As_2Te_3\}_{0.14}$) and the appearance of homopolar defective Ge-Ge bonds, respectively.

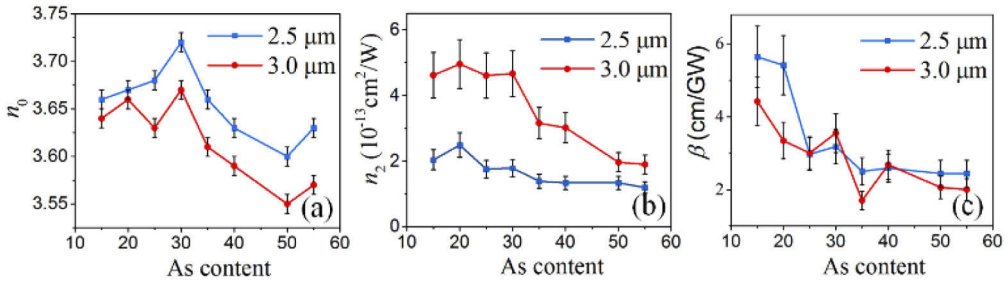


**Fig. 3.** (a) Linear refractive index, (b) nonlinear refractive index and (c) two-photon absorption coefficient as a function of As content in mol% at 2.5 μm (blue) and 3.0 μm (red).

In Fig. 3(b), the evolution of $n_2$ does not exhibit clear threshold behaviors, probably due to the relatively larger error in the measurement of the nonlinearity on one hand. On the other hand, $n_2$ might be more relevant to $E_g$ since the ratio of 3.0 μm wavelength photon energy $hv$ over $E_g$ steps from 0.53 to 0.50 at x = 30 and 35 which is located at the peak and the sharp declining tail respectively of the two-photon resonance effect (as shown in Fig. 5(a) below). By contrast, the $hv/E_g$ ratios of 2.5 μm wavelength range between 0.58-0.7 where $n_2$ slowly change along the ratios so as the $n_2$ keep almost still at 2.5 μm. Therefore, $n_2$ exhibits a sharp decrease in the glass with As content from x = 30 to 35 at 3.0 μm as shown in Fig. 3(b).

In Fig. 3(c) the two-photon coefficient $\beta$ generally exhibits larger values at Te-rich region whilst it becomes smaller in Te-poor glasses for both 2.5 and 3.0 μm. Nevertheless, an exceptional minimum $\beta$ value is observed in $Ge_{10}As_{35}Se_{55}$ ($\{GeTe_2\}_{0.1}$-$\{AsTe\}_{0.35}$) near chemically stoichiometric composition, implying that the less number of defective bonds near the stoichiometric compositions is favorite to achieve lower nonlinear absorption in the glasses, although the difference of the $\beta$ values is not so much.

The semi-empirical Miller's rule demonstrates the relation between the linear and nonlinear susceptibility $\chi^{(3)}$ written as [35],

$$\chi^{(3)} = \frac{n_2 n_0^2}{0.0395} = \alpha \left[ \frac{(n_0^2 - 1)}{4\pi} \right]^4 \tag{5}$$

where $\chi^{(3)}$ is the third order susceptibility in esu; $\alpha$ is the Miller's coefficient for chalcogenide glass. The main panels of Figs. 4(a) and (b) plot $\chi^{(3)}$ versus $[(n_0{}^2\text{-}1)/4\pi]^4$ at 2.5 and 3.0 μm, respectively, where the fitting based on Eq. (5) are exhibited (dashed lines) . The slope $\alpha$ of the dashed lines are used to determine the dependence of experimental $n_2$ on $n_0$ as shown in the insets. Good linear relation is achieved between linear and nonlinear susceptibility that obeys Miller's rule.

Optical Materials EXPRESS

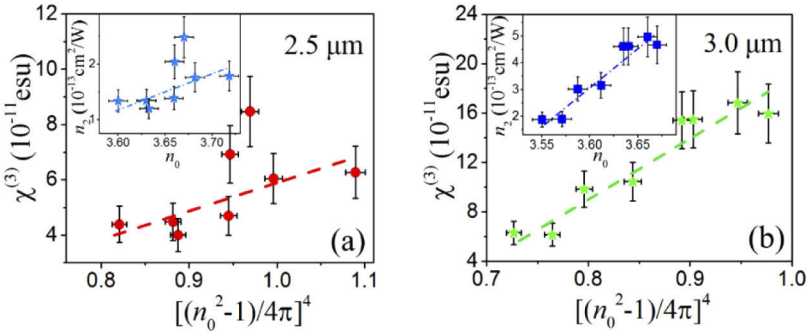


**Fig. 4.** Variation of the nonlinear susceptibility versus $(n_0{}^2\text{-}1)/4\pi$. Dashed lines are the theoretical fitting based on Eq. (5) at (a) 2.5 μm, and (b) 3.0 μm. The inset is the dependence of experimental $n_2$ on $n_0$.

Sheik-Bahae *et.al*. [36] have derived universal model to anticipate the dispersion of $n_2$ for direct-gap semiconductors. Meanwhile, a different model was suggested by Dinu *et.al*. [37] for indirect-gap semiconductors. Figure 5(a) shows that the theoretical prediction of $n_2$ from the Sheik-Bahae's model (solid line) is in satisfactory agreement to the Z-scan results with the maximum $n_2$ located at $h\nu/E_g \approx 0.54$ due to the enhancement of two-photon resonance effect. Meanwhile, the two-photon absorption $\beta$ is shown in Fig. 5(b), where the experimental result somehow resembles that predicted by Sheik-Bahae's model although there is a relatively big mismatch. This is mainly due to the fact that, it is much easier to produce more defective bonds in Te-based glasses [28], and these defective bonds tend to form intermediate states in the bandgap of $Ge_{10}As_xTe_{90-x}$, leading to additional nonlinear absorption so that $\beta$ does not vanish at half bandgap energy but remains significant. This also cause poor figure of merit (*FOM*) as listed in Table 1 that is impedible for nonlinear integrated photonic applications. Nevertheless, our experimental results seem to deviate from the Dinu's model.

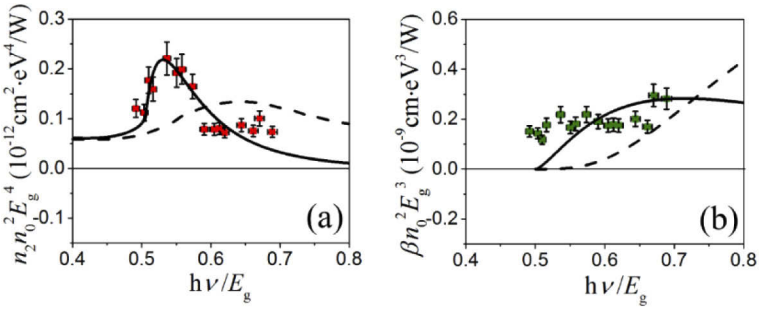


**Fig. 5.** (a). The behavior of normalized $n_2$ as a function of $h\nu/E_g$. (b) The behavior of normalized two photon absorption as a function of $h\nu/E_g$. The squares are the experimental data, the solid line are the fitting curves based on Sheik-Bahae's model and the dashed lines are Dinu's model.

## 4. Summary

In summary, we found that, the nonlinear optical index $n_2$ of $Ge_{10}As_xTe_{90-x}$ measured at 3.0 μm is larger than that at 2.5 μm because of the two-photon resonance effect, and a maximum nonlinear index is $4.96 \times 10^{-13}$ cm$^2$/W at composition of $Ge_{10}As_{20}Te_{70}$. We also analyzed the evolution of $n_0$, $n_2$ and $\beta$ as a function of As content. It is found that, both maximum $n_0$ and minimum $\beta$ are in

Optical Materials EXPRESS

the glasses close to the stoichiometric composition, whilst $n_2$ is more relevant to the variation of bandgap energies. While the data set of the $n_2$ can be well fitted by the direct-gap semiconductor model provided by Sheik-Bahae, the evolution of $\beta$ also follow variation trend described by Sheik-Bahae's model, but do not extend far enough to confirm the consistency although the overall trend indicates a reasonable correlation exists. The inconsistency of $\beta$ might be due to the absorption from the intermediate states formed by the large amount of defective bonds existed in the Te-based glasses. Nevertheless, large optical nonlinearity around $10^{-13}$ $cm^2/W$, which is one/two order larger than that in S- and Se-based chalcogenide glasses, makes it promising for mid- and far-infrared nonlinear processing such as supercontinuum and comb generation. Meanwhile the large linear refractive index of $Ge_{10}As_xTe_{90-x}$ glasses (3.60~3.72) promises strengthened light confining and manipulating capabilities that are crucial for long wave light operation. Less defective glasses need to be sought around chemically stoichiometric compositions of Te-based glasses with aims to lower two-photon and intermediate state absorptions and thus improve *FOM* of integrated photonic devices.

## Funding

National Natural Science Foundation of China (61575086, 61775109); 3315 Innovation Team in Ningbo City; the K. C. Wong Magna Fund in Ningbo University; Research Grants Council, University Grants Committee (8770006, 9048150); State Key Lab of Terahertz and Millimeter Waves (9360130, 9448001, 9605002); City University of Hong Kong Internal Grants (7005064, 7200572, 9610453).

## Acknowledgements

This work is supported by the Natural Science Foundation of China (Grant No. 61775109, 61575086); 3315 Innovation Team in Ningbo City, Zhejiang Province, China; the K. C. Wong Magna Fund in Ningbo University, China; Research Council of Hong Kong (Grant No. 9048150, 8770006); State Key Lab of Terahertz and Millimeter Waves, City University of Hong Kong, Hong Kong SAR, China (Grant No. 9360130, 9605002, 9448001); City University of Hong Kong Internal Grants (Grant No. 9610453, 7005064, 7200572).

## Disclosures

The authors declare no conflicts of interest.

## References

1. A. Zakery and S. R. Elliott, *Optical Nonlinearities in Chalcogenide Glasses and their Applications* (Spinger, 2007)
2. V. G. Ta'eed, N. J. Baker, L. B. Fu, K. Finsterbusch, M. R. E. Lamont, D. J. Moss, H. C. Nguyen, B. J. Eggleton, D. Y. Choi, S. Madden, and B. Luther-Davies, "Ultrafast all-optical chalcogenide glass photonic circuits," Opt. Express **15**(15), 9205–9221 (2007).
3. F. Charpentier, B. Bureau, J. Troles, C. Boussard-Plédel, K. M.-L. Pierrès, F. Smektala, and J.-L. Adam, "Infrared monitoring of underground $CO_2$ storage using chalcogenide glass fibers," Opt. Mater. **31**(3), 496–500 (2009).
4. J. S. Sanghera and I. D. Aggarwal, "Active and Passive Chalcogenide Glass Optical Fibers for IR Applications: A Review," J. Non-Cryst. Solids **256-257**(16), 6–16 (1999).
5. C. R. Petersen, U. Moller, I. Kubat, B. Zhou, S. Dupont, J. Ramsay, T. Benson, S. Sujecki, N. Abdel-Moneim, Z. Tang, D. Furniss, A. Seddon, and O. Bang, "Mid-infrared supercontinuum covering the 1.4-13.3 μm molecular fingerprint region using ultra-high NA chalcogenide step-index fibre," Nat. Photonics **8**(11), 830–834 (2014).
6. X. Gai, D.-Y. Choi, S. Madden, Z. Yang, R. Wang, and B. Luther-Davies, "Supercontinuum generation in the mid-infrared from a dispersion-engineered $As_2S_3$ glass rib waveguide," Opt. Lett. **37**(18), 3870–3872 (2012).
7. Y. Yu, B. Zhang, X. Gai, C. Zhai, S. Qi, W. Guo, Z. Yang, R. Wang, D. Y. Choi, S. Madden, and B. Lutherdavies, "1.8-10 μm mid-infrared supercontinuum generated in a step-index chalcogenide fiber using low peak pump power," Opt. Lett. **40**(6), 1081–1084 (2015).
8. Y. Yu, X. Gai, P. Ma, D.-Y. Choi, Z. Yang, R. Wang, S. Debbarma, S. J. Madden, and B. Luther-Davies, "A broadband, quasi-continuous, mid-infrared supercontinuum generated in a chalcogenide glass waveguide," Laser Photonics Rev. **8**(5), 792–798 (2014).

Optical Materials EXPRESS


9. A. Prasad, C.-J. Zha, R.-P. Wang, A. Smith, S. Madden, and B. Luther-Davies, "Properties of GexAsySe1-x-y glasses for all-optical signal processing," Opt. Express **16**(4), 2804–2815 (2008).
10. K. Ogusu, J. Yamasaki, S. Maeda, M. Kitao, and M. Minakata, "Linear and nonlinear optical properties of Ag-As-Se chalcogenide glasses for all-optical switching," Opt. Lett. **29**(3), 265–267 (2004).
11. G. Lenz, J. Zimmermann, T. Katsufuji, M. E. Lines, H. Y. Hwang, S. Spalter, R. E. Slusher, S. W. Cheong, J. S. Sanghera, and I. D. Aggarwal, "Large Kerr effect in bulk Se-based chalcogenide glasses," Opt. Lett. **25**(4), 254–256 (2000).
12. J. M. Harbold, F. O. Ilday, F. W. Wise, J. S. Sanghera, V. Q. Nguyen, L. B. Shaw, and I. D. Aggarwal, "Highly nonlinear As-S-Se glasses for all-optical switching," Opt. Lett. **27**(2), 119–121 (2002).
13. S. Dai, F. Chen, Y. Xu, Z. Xu, X. Shen, T. Xu, R. Wang, and W. Ji, "Mid-infrared optical nonlinearities of chalcogenide glasses in Ge-Sb-Se ternary system," Opt. Express **23**(2), 1300–1307 (2015).
14. M. Olivier, J. C. Tchahame, P. Němec, M. Chauvet, V. Besse, C. Cassagne, G. Boudebs, G. Renversez, R. Boidin, and E. Baudet, "Structure, nonlinear properties, and photosensitivity of $(GeSe_2)_{100-x}(Sb_2Se_3)_x$ glasses," Opt. Mater. Express **4**(3), 525 (2014).
15. T. Halencovic, J. Gutwirth, T. Kuriakose, M. Bouska, and V. Nazabal, "Linear and nonlinear optical properties of co-sputtered Ge-Sb-Se amorphous thin films," Opt. Lett. **45**(6), 1523–1526 (2020).
16. K. Tanaka and K. Shimakawa, *Amorphous Chalcogenide Semiconductors and Related Materials* (Springer, 2011)
17. R. P. Wang, *Amorphous Chalcogenides : Advances and Applications* (Pan Stanford Publishing, 2014)
18. P. Sharma and S. C. Katyal, "Effect of deposition parameters on the optical energy gap and refractive index of a-Ge–Se–Te thin films," Philos. Mag. **88**(17), 2549–2557 (2008).
19. J. Akola and R. O. Jones, "Structural phase transitions on the nanoscale: The crucial pattern in the phase-change materials $Ge_2Sb_2Te_5$ and GeTe," Phys. Rev. B **76**(23), 235201 (2007).
20. J. A. Savage, "Glass forming region and DTA survey in the Ge-As-te memory switching glass system," J. Mater. Sci. **6**(7), 964–968 (1971).
21. M. A. Popescu, *Non-Crystalline Chalcogenides* (Kluwer Academic Publishers, 2000)
22. M. Sheik Bahae, A. A. Said, T. H. Wei, D. J. Hagan, and E. W. Van Stryland, "Sensitive measurement of optical nonlinearities using a single beam," IEEE J. Quantum Electron. **26**(4), 760–769 (1990).
23. M. Yin, H. P. Li, S. H. Tang, and W. Ji, "Determination of nonlinear absorption and refraction by single Z-scan method," Appl. Phys. B **70**(4), 587–591 (2000).
24. B. Gu, J. Wang, J. Chen, Y. X. Fan, J. P. Ding, and H. T. Wang, "Z-scan theory for material with two- and three-photon absorption," Opt. Express **13**(23), 9230–9234 (2005).
25. P. Hawlová, F. Verger, V. Nazabal, R. Boidin, and P. Němec, "Accurate Determination of Optical Functions of Ge-As-Te Glasses via Spectroscopic Ellipsometry," J. Am. Ceram. Soc. **97**(10), 3044–3047 (2014).
26. J. Tauc and A. Menth, "States in the gap," J. Non-Cryst. Solids **8-10**(8), 569–585 (1972).
27. T. Wang, X. Gai, W. Wei, R. Wang, Z. Yang, X. Shen, S. Madden, and B. Luther-Davies, "Systematic z-scan measurements of the third order nonlinearity of chalcogenide glasses," Opt. Mater. Express **4**(5), 1011–1022 (2014).
28. N. Sharma, S. Sharda, S. C. Katyal, V. Sharma, and P. Sharma, "Effect of Te on linear and non-linear optical properties of new quaternary Ge-Se-Sb-Te chalcogenide glasses," Electron. Mater. Lett. **10**(1), 101–106 (2014).
29. M. Kastner, "Bonding Bands, Lone-Pair Bands, and Impurity States in Chalcogenide Semiconductors," Phys. Rev. Lett. **28**(6), 355–357 (1972).
30. R. Holomb, V. Mitsa, S. Akyuz, and E. Akalin, "New ring-like models and ab initio DFT study of the medium-range structures, energy and electronic properties of $GeSe_2$ glass," Philos. Mag. **93**(19), 2549–2562 (2013).
31. J. M. Harbold, F. O. Ilday, F. W. Wise, and B. G. Aitken, "Highly nonlinear Ge-As-Se and Ge-As-S-Se glasses for all-optical switching," IEEE Photonics Technol. Lett. **14**(6), 822–824 (2002).
32. S. Sen, E. L. Gjersing, and B. G. and Aitken, "Physical properties of $Ge_xAs_{2x}Te_{100-3x}$ glasses and Raman spectroscopic analysis of their short-range structure," J. Non-Cryst. Solids **356**(41-42), 2083–2088 (2010).
33. K. Sútorová, P. Hawlová, L. Prokes, P. Němec, R. Boidin, and J. Havel, "Laser desorption ionization time-of-flight mass spectrometry of Ge-As-Te chalcogenides," Rapid Commun. Mass Spectrom. **29**(5), 408–414 (2015).
34. H. Pan, Z. Yang, Y. Chen, R. Wang, and X. Shen, "X-ray photoelectron spectra of Ge-As-Te glasses," AIP Adv. **8**(7), 075208 (2018).
35. R. W. Boyd, *Nonlinear Optics, second Edition* (Academic Press Inc., 2003)
36. M. Sheik Bahae, D. J. Hagan andE, and W. Van Stryland, "Dispersion and band-gap scaling of the electronic Kerr effect in solids associated with two-photon absorption," Phys. Rev. Lett. **65**(1), 96–99 (1990).
37. M. Dinu, "Dispersion of phonon-assisted nonresonant third-order nonlinearities," IEEE J. Quantum Electron. **39**(11), 1498–1503 (2003).